

Fabrication and characterization of copper(II)-chitosan complexes as antibiotic-free antibacterial biomaterial



Lukas Gritsch^{a,b}, Christopher Lovell^b, Wolfgang H. Goldmann^c, Aldo R. Boccaccini^{a,*}

^a Institute of Biomaterials, University of Erlangen-Nuremberg, Cauerstraße 6, 91058 Erlangen, Germany

^b Lucideon Ltd., Queens Road, Penkhull, Stoke-on-Trent, Staffordshire, ST4 7LQ, UK

^c Department of Biophysics, University of Erlangen-Nuremberg, Henkestrasse 91, 91052 Erlangen, Germany

ARTICLE INFO

Keywords:

Chitosan
Copper
Chelation
Therapeutic ions
Antimicrobial materials
Antibiotic-free

ABSTRACT

We produced and characterized copper(II)-chitosan complexes fabricated via in-situ precipitation as antibiotic-free antibacterial biomaterials. Copper was bound to chitosan from a dilute acetic acid solution of chitosan and copper(II) chloride exploiting the ability of the polysaccharide to chelate metal ions. The influence of copper(II) ions on the morphology, structure and hydrophobicity of the complexes was evaluated using scanning electron microscopy, energy-dispersive X-ray spectroscopy, attenuated total reflectance Fourier transform infrared spectroscopy and static contact-angle measurements. To assess the biological response to the materials, cell viability and antibacterial assays were performed using mouse embryonic fibroblasts and both Gram-positive and –negative bacteria. Combined analysis of cell and bacterial studies identified a threshold concentration at which the material shows outstanding antibacterial properties without significantly affecting fibroblast viability. This key outcome sets copper(II)-chitosan as a promising biomaterial and encourages further investigation on similar systems toward the development of new antibiotic-free antibacterial technologies.

1. Introduction

Bacterial resistance to antimicrobial agents, especially antibiotics, is a challenge that has been recently recognized and addressed by the authorities all over the world as an emerging threat to humanity (Michael, Dominey-Howes, & Labbate, 2014; O'Neill, 2014). Risks of regression to a situation of high death-by-infection rates, typical of the pre-antibiotic era, seems to be a close reality which demands a strong multidisciplinary counter attack from the scientific community with the development of new antimicrobial technologies that kill bacteria without triggering unwanted resistances (Ventola, 2015a, 2015b). In this regard, the engineering of biomaterials is one strategy that has the potential to significantly reduce the risk of infections in all healthcare disciplines. Material technologies used in medical devices, such as for coatings of implants, wound dressing platforms or tissue engineering scaffolds need not only to provide an effective therapeutic solution for patients, but they should also possess antimicrobial properties that can inhibit the growth of bacteria, fungi and other microorganisms (O'Brien, 2011).

Among others, one material that has attracted the attention of recent research concerning the development of antibacterial biomaterials is chitosan. This interest is due to the plethora of beneficial properties

that chitosan has, above all its intrinsic antibacterial and antifungal activity (Kong, Chen, Xing, & Park, 2010; Munoz-Bonilla, Cerrada, & Fernandez-Garcia, 2014). Moreover, chitosan possesses several other remarkable properties that make it a unique candidate in the development of a broad range of biomedical devices. Key features of chitosan as biomaterial are its cytocompatibility, mucoadhesion and haemostatic activity (Kim, 2011). Many beneficial properties are related to the presence of protonatable amino groups within the d-glucosamine moieties (Munoz-Bonilla et al., 2014). These amino groups are exposed from the original units of acetylglucosamine of chitin (i.e. the precursor of chitosan) via deacetylation of the polysaccharide. In other words, the more acetylglucosamine units that are deacetylated, the more reactive amino groups are exposed and available for reaction. The degree of deacetylation (DDA) of chitosan can easily be modified, as a consequence it is possible to tailor the aforementioned properties of the material via relatively straightforward chemical procedures. Furthermore, chitosan offers significant economic advantages over other similar materials since it is a readily available by-product of the ichthyic industry. The main drawbacks of chitosan concern its potential allergenicity and relatively poor mechanical properties (Kim, 2011; Munoz-Bonilla et al., 2014), though the latter may be improved via crosslinking techniques (Rivero, García, & Pinotti, 2013). A strong and

* Corresponding author.

E-mail addresses: lukas.gritsch@fau.de (L. Gritsch), christopher.lovell@lucideon.com (C. Lovell), wgoldmann@aol.com (W.H. Goldmann), aldo.boccaccini@fau.de (A.R. Boccaccini).

beneficial property of chitosan is its ability to chelate with a broad spectrum of metal ions, in particular transition elements. The chelating ability of chitosan is well-documented and has been extensively studied (Guibal, 2004; Qin, 1993; Rhazi et al., 2002). The mechanisms of action toward several metallic ions and the molecular changes that occur as a consequence of the complexation have been well characterized via a broad spectrum of techniques, including potentiometry, UV spectroscopy and circular dichroism (Rhazi et al., 2002). The proposed mechanism for chitosan's chelating ability concerns the formation of coordination bonds with metal ions via side amino and hydroxyl groups (Guibal, 2004; Guibal, Vincent, & Navarro, 2014; Qin, 1993; Qu et al., 2011).

A variety of chitosan forms (e.g. membranes, sponges, microspheres) have been considered to exploit the chelation between chitosan and metal ions in new advanced materials (Guibal, 2004; Guibal et al., 2014; Mekahlia & Bouzid, 2009). While the main focus of research so far has been the development of convenient, cost effective and environmentally friendly chitosan-based waste water treatments, sensors and new catalysts for industry, alternative applications have started to emerge. For example, there is growing interest toward the exploitation of chitosan to entrap specific antimicrobial ions in order to design a new generation of antibacterial materials, mainly for high-tech packaging applications. Wang et al. (Wang, Du, Fan, Liu, & Hu, 2005), for instance, prepared antibacterial chitosan-metal complexes. The ions chosen in their study were Cu(II), Zn(II) and Fe(II). The materials were characterized via Fourier transform infrared spectroscopy (FTIR), X-ray diffraction (XRD), atomic absorption spectroscopy (AAS) and elemental analysis, confirming a successful chelation and an optimal sustained release of ions. Bacterial (Gram-positive and Gram-negative) and fungi cultures confirmed significant inhibitory effects. Similar studies were carried out by Ma et al. (Ma, Zhou, & Zhao, 2008), who synthesized chitosan-silver complexes, and by Higazy et al. (Higazy, Hashem, ElShafei, Shaker, & Hady, 2010), who investigated the efficacy of chitosan and chitosan-silver as antibacterial packaging additives. However, these reports focus only on chitosan as a wrapping material. The unexplored potential outcomes of these chelation-based techniques are vast and promising and go way beyond the usage of modified chitosan for packaging. Metal ions within the chitosan matrix can give the polysaccharide a range of diverse and valuable properties for applications in medicine. For instance, one of the most interesting aspects of the chelation ability of chitosan is that many of the ions that form complexes belong to a family of biologically active agents: therapeutic metal ions (TMIs) (Mourino, Cattalini, & Boccaccini, 2012). TMIs interact with a number of biological structures and metabolic systems and are able to have a positive effect on the regeneration of tissue when interacting with target mammalian cells, while inhibiting the growth of prokaryotes. Their activity could offer a viable alternative to expensive and delicate biomolecules (such as growth factors) that also raise concerns with regards to their safety (Mourino et al., 2012). However, the literature has very few investigations of chitosan-metal based materials as platforms for biomedical applications. For example, a recent paper reported the fabrication of a new kind of bone fixation device based on chitosan chelating iron ions (Qu et al., 2011). To our knowledge, no previous study has addressed the combination of chitosan with TMIs to achieve a combination of biocompatibility and antimicrobial activity.

In this work we present our initial study on the preparation of a copper(II)-chitosan biomaterial that could be used in the fabrication of functional coatings and tissue engineering scaffolds with intrinsic antimicrobial activity. Copper (II) is a TMI that provides a rapid antimicrobial action without the risk of resistance development (ICA, 2017; Vincent, Hartemann, & Engels-Deutsch, 2016) and, at the same time, has the ability to modulate angiogenesis (Xie & Kang, 2009), a crucial challenge of current tissue engineering technologies. Moreover, copper is naturally present in the human body, contrary, for instance, to silver. Copper(II)-chitosan samples were characterized by scanning electron

microscopy (SEM), energy dispersive X-ray spectroscopy (EDX), static contact-angle measurements and attenuated total reflectance Fourier transform infrared spectroscopy (ATR-FTIR). Biological characterizations using mouse embryonic fibroblasts (MEFs) and two strains of bacteria, Gram-positive *Staphylococcus Carnosus* and Gram-negative *Escherichia Coli*, were also performed to identify an optimal window of action within which the material could inhibit or kill bacteria without significantly harming mammalian cells.

2. Experimental

2.1. Materials

Medium molecular weight chitosan from Sigma-Aldrich, Germany (DDA ~75–85%, MW ~190–310 kDa, viscosity 200–800 cP) was chosen due to its DDA, optimal to load the desired amount of copper ions. Moreover, the medium molecular weight ensures sufficient integrity and mechanical strength. The properties of chitosan provided by the supplier are considered reliable thanks to previous projects conducted on the same material (Liverani et al., 2017). Anhydrous copper (II) chloride (purity 99%) was purchased from Sigma Aldrich, Germany. Glacial acetic acid (AcOH) and sodium hydroxide (NaOH) were obtained from VWR, Germany. All reagents were of analytical grade and were used without any further purification.

2.2. Preparation of copper(II)-chitosan complexed gels via *in situ* precipitation

Complexed gels of chitosan and copper were prepared via *in situ* precipitation method, adapting a previously described protocol (Qu et al., 2011). Chitosan was dissolved in a diluted acetic acid solution (2% v/v) at a concentration of 2% w/v under constant stirring at 40 °C. After complete dissolution of chitosan, various amounts of CuCl₂ were added and left to disperse homogeneously for one hour. Four samples were fabricated (Table 1), varying the mass of copper salt in the solution (m_{CuCl₂}) according to the theoretical amount of free amino groups of chitosan, as follows:

$$m_{CuCl_2} = X \cdot MM_{CuCl_2} \cdot \frac{m_{Chi}}{MM}$$

$$\overline{MM} = DDA \cdot MM_{glu} + (1 - DDA) \cdot MM_{N-acetylglu} = 187.578 \text{ g/mol}$$

The degree of deacetylation used for the calculation is the average of the given range (DDA ~80%). m_{Chi} is the amount of chitosan in grams, MM_{CuCl₂} is the molecular mass of copper chloride (134.45 g/mol), MM_{glu} and MM_{N-acetylglu} the molecular weights of glucosamine (179.17 g/mol) and N-acetylglucosamine moieties respectively (221.21 g/mol). Finally, X is a fraction corresponding to the desired ratio of Cu(II) ions to free amino groups (Cu²⁺:NH₂).

The solutions were then cast in a 24-multiwell plate and overlaid with aqueous 0.1 M NaOH solution for 4 h. Subsequently, the gels were rinsed with deionized water until complete neutralization of the pH and then dried in an oven at 60 °C for 2 h. Following this protocol, bright blue disc shaped samples were obtained (Fig. 1). The series of samples given in Table 1 are labelled according to the weight percentage of copper ions. Samples produced following the same protocol, but without copper, were used as control and are labelled "Chi". A qualitative morphological evaluation of the gels was performed via optical

Table 1
Quantities of copper added to chitosan and corresponding sample labelling.

Label	Chi	CuChi3	CuChi6	CuChi12	CuChi18
CuCl ₂ amount (mg)	0,0	12,5	25,0	50,0	75,0
X (%)	0	3	6	12	18
Cu ²⁺ :NH ₂	–	1:33	1:17	1:8	1:6

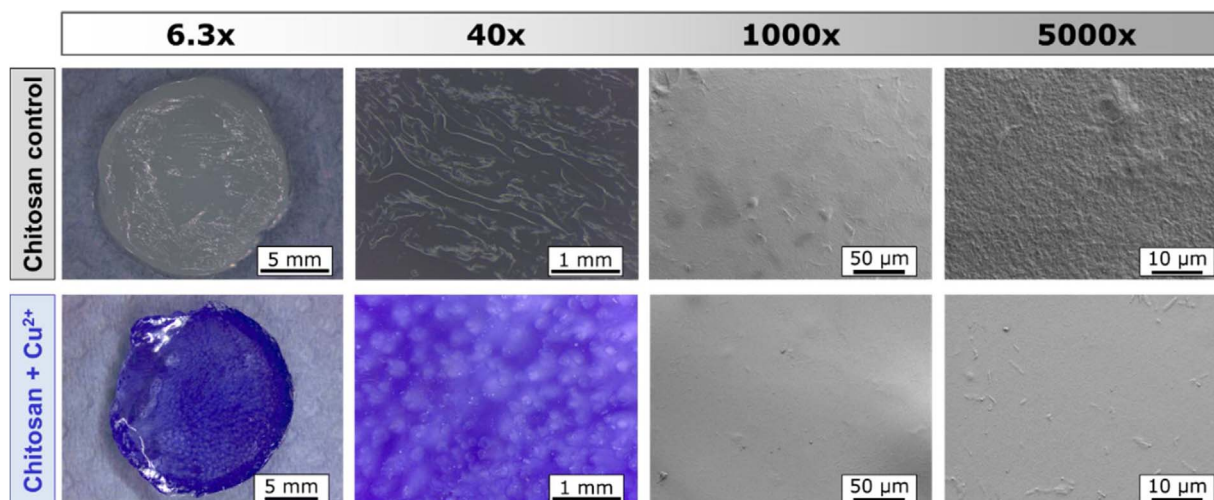


Fig. 1. Optical and electron microscopy images of chitosan and copper(II)-chitosan (CuChi12) at different magnifications. The samples are characterized by a homogeneous and smooth surface.

(Leica M50 and IC80) and scanning electron (LEO 435 VP, LEO Electron Microscopy Ltd., Cambridge, UK and Ultra Plus, Zeiss, Jena, Germany) microscopies in order to assess the extent of homogeneous complexation of copper ions in the polymer matrix.

2.3. EDX spectroscopy

Energy-Dispersive X-ray spectroscopy (EDX) was used to confirm the presence of copper in the samples. Both punctual and cumulative spectra were acquired from various samples and from multiple positions for each sample using a Silicon Drift Detector (SDD) X-Max^N, Oxford Instruments, UK.

2.4. FTIR spectroscopy

The acquisition of infrared spectra of all samples was carried out using a Shimadzu IRAffinity-1S (Shimadzu Corp, Japan) equipped with LabSolution IR software and a Quest ATR GS10801-B single bounce diamond accessory (Specac Ltd, England). Data (40 scans, resolution of 4 cm^{-1}) were collected in the mid-IR region ($4000\text{--}400\text{ cm}^{-1}$) after air-drying of samples previously stocked in deionized water.

2.5. Wettability

Contact-angle measurements were performed at room temperature using a Krüss DSA30 Drop Shape Analysis System (Krüss GmbH, Germany) on hydrated copper(II)-chitosan samples with amounts of copper, as described in Table 1. The procedure involved deposition of a $3\text{ }\mu\text{L}$ deionized water droplet on the surface of the sample, the subsequent acquisition of an image of the drop and the computation of the contact-angles (both left and right) for six consecutive times within 3 s using the software DSA4 (Krüss GmbH, Germany).

The procedure was repeated four times in different positions on the sample. In order to assess the variation in time of the contact-angle, the same procedure was repeated for ten times every thirty seconds from $t=0$ to five minutes after the deposition.

2.6. Cell biology

2.6.1. Cell seeding and culture

Cell line Mouse Embryonic Fibroblasts (MEFs) were cultured in a polystyrene flask using Dulbecco modified Eagle medium (DMEM) supplemented with 10% (v/v) of fetal bovine serum (FBS) and 1% (v/v) of antibiotic and antimycotic PenStrep (all reagents purchased from

Gibco[®], Germany). A monolayer of MEF close to confluence was detached using trypsin/1 mM ethylenediaminetetraacetic (EDTA) (Life Technologies, Germany) in PBS. Then the trypsin was inactivated by dilution in fresh DMEM. Cells were counted via the trypan blue exclusion method (Sigma-Aldrich, Germany) before seeding. Samples were UV sterilized for one hour and then preconditioned for 24 h in DMEM prior to contact with cells. 100.000 cells per well were seeded and incubated in a humidified atmosphere of 95% relative humidity and 5% CO_2 , at $37\text{ }^\circ\text{C}$ for 24 h. Afterwards, specimens were immersed in the culture medium of each well by using polyethylene terephthalate (PET) cell culture inserts (Transwell[®] by Corning[®], Germany) and incubated for further 24 h before testing. The inserts were equipped with a membrane that permits mass exchange keeping the sample and the cells separated. In this way the effect of the release of ions from the sample can be isolated and evaluated without the interference of other material properties that could affect the cell growth, such as stiffness or surface topography. Cells cultured with pure medium were considered as control. Three independent cultures with four samples each were performed for statistical significance ($n = 3 \times 4$).

2.6.2. Mitochondrial activity

The response of the cells to copper-modified chitosan gels was evaluated after a further 24 h of culture by performing a mitochondrial activity colorimetric assay (WST-8 assay kit, Sigma-Aldrich, Germany) that quantifies the enzymatic conversion of tetrazolium salt. Culture medium was removed completely from the wells, samples were disposed and the cells were washed with PBS. Freshly prepared culture medium containing 1% v/v WST-8 assay kit was added and the cells were incubated for 3 h. Subsequently, 100 μL of supernatant from each sample was transferred into a well of a 96 well-plate and the absorbance at 450 nm was measured with a micro plate reader (PHOMo Autobio, Labtec Instruments co. Ltd. China). From the acquired absorbance measurements, cell viability was calculated computing the absorbance of each specimen (A_i) and the one of the respective positive control (A_0):

$$\text{cell viability}(\%) = \frac{A_i}{A_0} \times 100$$

2.6.3. Cell staining

To assess the viability of cells, live staining was performed by calcein AM (calcein acetoxymethyl ester, Invitrogen, USA) after culture, and nuclei were visualized by blue nucleic acid stain, DAPI (4',6-diamidino-2-phenylindole, dilactate, Invitrogen, USA) which preferentially

bind to A (Adenine) and T (Thymine) bases within DNA. The images of calcein-DAPI were taken with a fluorescence microscope (FM) (Axio Observer D1, Carl Zeiss Microimaging GmbH, Germany).

2.7. Bacterial culture

A direct contact bacterial assay was performed on all types of copper modified chitosan samples in order to assess their ability to inhibit bacterial growth over time. Prior to use, all glassware used in the study was sterilized in autoclave and the samples were sterilized by UV irradiation for 1 h and then preconditioned in sterile PBS (Gibco, Germany) overnight. Isolated colonies of Gram-negative *Escherichia Coli* and Gram-positive *Staphylococcus Carnosus* selected as test strains were cultured in a nutrient broth (LB broth #968.1, Carl Roth GmbH) overnight at 100 rpm and 37 °C in order to obtain fresh bacteria suspension suitable for inoculation. On the second day, the fresh bacteria suspension was diluted to an optical density (600 nm, Eppendorf BioPhotometer) of 0.015. Subsequently 50 μL of the diluted suspension was deposited on the specimens. Optical density was used as an estimation of the colony forming units (CFU) in the suspension (Sutton, 2011). Preliminary experiments verified that by using this protocol the bacteria loaded are in the log phase. Once the value of OD was selected it was kept constant throughout all experiments in order to guarantee reproducibility. At 1, 3 and 6 h the medium was transferred onto a fresh agar (LB Agar (Lennox), Lab M Ltd.) plate and incubated overnight in order to visualize the bacterial growth and/or inhibition. High resolution images of the agar plates were taken with a digital camera (Nikon D90) and further processed according to the following procedure: the original image was first desaturated (luminosity shades of gray algorithm, GIMP open source software) and then a threshold was manually set via ImageJ (National Institutes of Health, USA) in order to produce clear contrast between black background pixels and white “bacterial pixels”. The percentage of the image area due to white pixels was considered a measure of the bacterial growth. This information results in an index that goes from 0 (=no area covered by bacteria) to 1 (=agar completely covered by bacteria). The test was performed in triplicate for statistical significance, independently grown bacterial strains were used.

2.8. Statistical analysis

All results are expressed as mean \pm standard deviation. Statistically significant differences have been assessed using either two tailed Student's *t*-test to compare two samples or one way ANOVA to compare multiple datasets ($p < 0.05$).

3. Results

3.1. Effect of copper(II) addition on chitosan structural characteristics

The EDX spectra displayed peaks related to the three main elements that constitute chitosan (carbon, nitrogen and oxygen) and a smaller peak that can be attributed to the presence of copper ions (Fig. 2). Furthermore, mappings across the sample revealed that the distribution of copper was homogeneous. Notably, the EDX results did not reveal any significant contamination neither from metal ions from unwanted sources (e.g. laboratory tools), nor residual chlorine due to the initial copper salt nor any sodium from the NaOH used to trigger the precipitation. After a linear baseline correction, the area of the copper L peak from various spectra ($n = 4$) was then normalized with respect to the carbon peak to obtain a preliminary and semi-quantitative evaluation of the amount of copper loaded in the samples. The resulting $\text{Cu}_{\text{KL}}/\text{C}_{\text{K}\alpha}$ ratio was found to increase proportionally to the amount of copper added to the chitosan, confirming increased chelation of copper ions (Table 2). At the same time, as control, the ratio between the carbon and the oxygen peak areas was calculated and it was seen to remain

constant for all the copper(II)-chitosan formulations.

Characteristic FTIR spectral bands of chitosan, as reported in literature (Cárdenas & Miranda, 2004; Qu et al., 2011), include, from higher to lower wavenumbers, a broad band around 3400 cm^{-1} related to the stretching of N–H and O–H bonds, including hydroxyls from residual water, two weaker bands caused by the stretching of C–H ($\sim 2900\text{ cm}^{-1}$), the peaks of amidic C=O bonds stretching ($\sim 1650\text{ cm}^{-1}$), N–H bending mode ($\sim 1600\text{ cm}^{-1}$), a peak at around 1400 cm^{-1} usually attributed either to the deformation of C–H (Cárdenas & Miranda, 2004) or the stretching of C–N (Qu et al., 2011) and finally a strong band, with various small peaks between 1100 and 1000 cm^{-1} , due to the stretching of the glycosidic bond C–O that connects the glucosamine monomers of chitosan (Kim, 2011).

Modifications to the structure of chitosan due to the chelation of copper ions caused shifts in wavenumber and changes in relative absorbance of specific spectral bands involved in the coordination between the polysaccharide and copper. In Fig. 3 a comparison is made between a control sample of bare chitosan and a *CuChi12* sample. However, no measurable differences were observed in the spectra of samples with different amounts of copper.

The principal variations that occur after the modification with copper(II) result as a consequence of the interaction between chitosan and the metal ions. A decrease in the relative absorbance of the 3300 cm^{-1} band, associated with $\nu_{\text{O-H}}$ and $\nu_{\text{N-H}}$, has been attributed to the participation of both amine and hydroxyl groups in the chelation (Qin, 1993; Qu et al., 2011), although a change in overall hydrophobicity and a decrease of residual water content from the control into the samples may also be a contributing factor. In addition to the reduction in absorbance of O–H and N–H stretching vibrations, a decrease in absorbance is also observed for amide and amine bands at respectively 1650 cm^{-1} and 1600 cm^{-1} . These observations have similarly been reported in the literature and provide further evidence for the involvement of these groups in complex formation (Mekahlia & Bouzid, 2009; Qu et al., 2011). Moreover the lineshape of the characteristic peak of the glycosidic bond at $\sim 1100\text{ cm}^{-1}$ changes as a consequence of the cross-coordination of copper(II) with adjacent chains of chitosan (Qu et al., 2011).

3.2. Wettability

In Fig. 4A droplet profiles for all analyzed samples are shown. From a first qualitative assessment it appears that no significant variation occurs in wettability as a consequence of the addition of copper. The values obtained for every type of sample are set within the $75\text{--}90^\circ$ range, implying a mildly hydrophobic behavior of chitosan and its copper-modified versions. By observing the histogram in Fig. 4B, reporting the angle values for all samples, the same conclusion can be drawn: the addition of copper does not change wettability with statistical significance ($p < 0.05$).

Although the behavior of the droplet on the samples appears relatively unchanged after deposition, a very different picture can be appreciated by monitoring the contact angle over time (Fig. 4B). While droplets on pure chitosan quickly reduce their angle from a starting value of $\sim 80^\circ\text{--}\sim 40^\circ$, this variation is drastically attenuated, if not completely absent, on all the samples modified with copper, regardless of the amount of added ions. After five minutes from the deposition of the water droplet the contact angle of the droplet on pristine chitosan fell to around half of its initial value. The most reasonable explanation for this behavior is that, as already discussed, the chelation of the same copper ion by two adjacent chitosan chains induces a crosslinking of the polysaccharide matrix which is capable of reducing cracks on the surface that cause sorption of water from the droplet to the inner part of the sample.

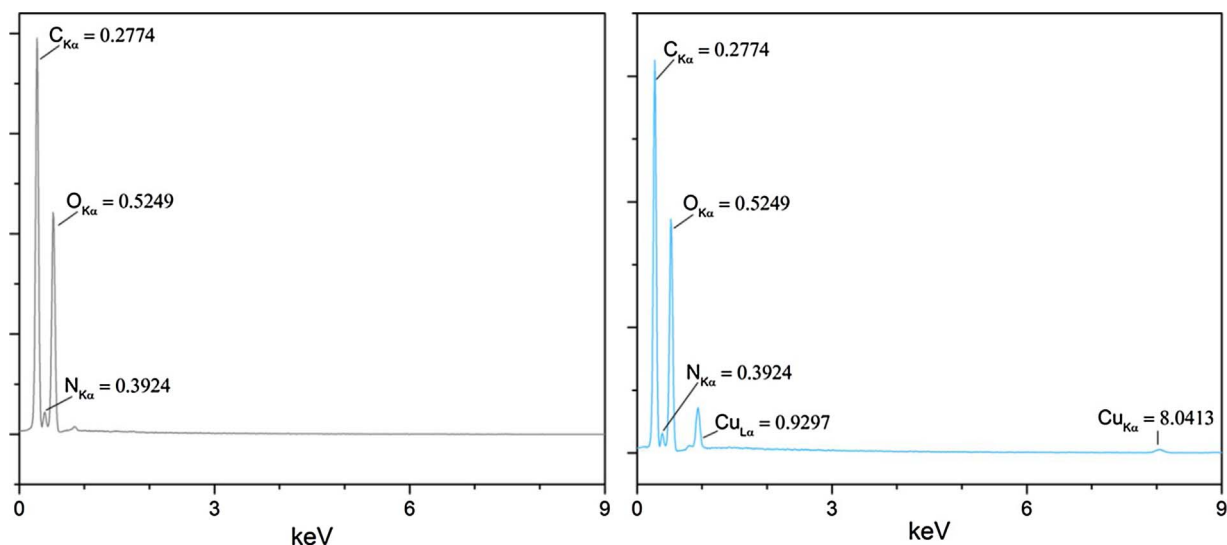


Fig. 2. EDX spectra confirming the presence of copper in CuChi12 samples and absence of contamination from reagents and/or other sources (right panel), compared to a chitosan control (left panel). Similar results are obtained with all other sample types. The $Cu_{L\alpha}$ of copper increase proportionally to the amount of copper added during preparation of the samples (Table 2).

Table 2

Ratios between the intensity of the copper L peak and the carbon peak of the EDX spectra of CuChi samples.

Sample	CuChi3	CuChi6	CuChi12	CuChi18
$Cu_{L\alpha}/C_{K\alpha}$ ratio (%)	3.3 ± 0.6	4.7 ± 1.0	9.6 ± 1.0	13.6 ± 2.2

3.3. Cell biology

Samples of each material, including a chitosan sample and a positive control, were biologically characterized using mouse embryonic fibroblasts (MEF) in order to establish possible cytotoxic effects due to the presence of copper(II) ions. The results of the WST-8 quantitative assay were consistent with the previously reported excellent cytocompatibility of chitosan (Nwe, Furuike, & Tamura, 2009; Sarasam & Madihally, 2005), but highlight cell viability levels that

gradually decrease with increasing copper content, as shown in Fig. 5A. Specifically, pure chitosan control samples without copper and samples with 3% copper(II) ions are characterized by cell viability values comparable to the positive control; the following variety of copper(II)-chitosan samples (i.e. 6%) still has a relatively positive value of ($75 \pm 7\%$). On the contrary, *CuChi12* and *CuChi18* reveal decreasing cell viability of ($55 \pm 8\%$) and ($48 \pm 2\%$) respectively. Especially for the last typology, the assessed values are below 50% of the positive control and are evidence of clear cytotoxic effects due to excessive levels of copper(II) ions expected to be present in the culture medium. The differences in cell viability between sample types are statistically significant for copper amounts higher than 3%. The morphology of the cells confirms the quantitative assessment and shows how the number of healthy and filopodia-rich fibroblasts tends to decrease with increasing amount of Cu(II), as can be seen from the fluorescence microscopy images presented in Fig. 5B. Again for pure chitosan, *CuChi3* and *CuChi6* the results of staining are comparable to the positive

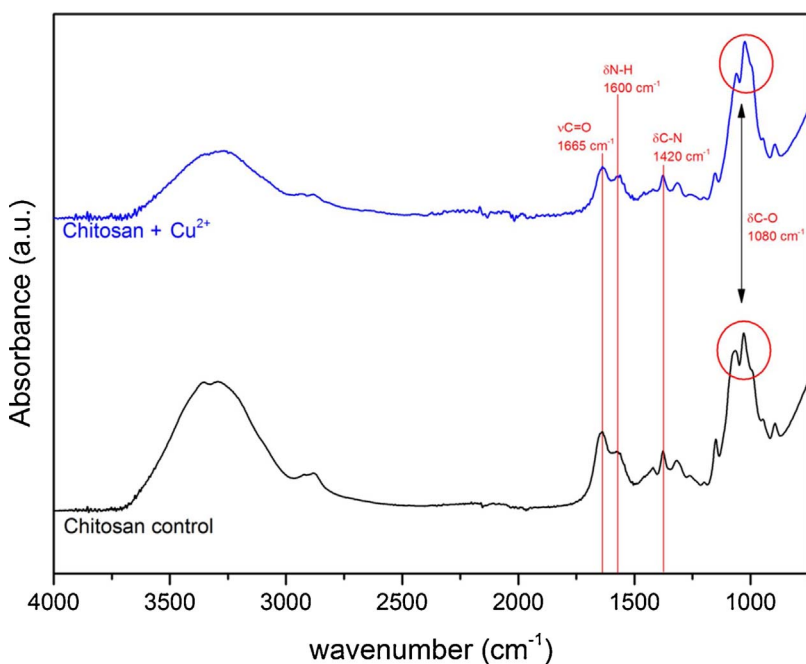


Fig. 3. Comparison between the ATR-FTIR spectra of pure chitosan and CuChi12 highlighting the main differences introduced by the copper doping. The sole CuChi12 spectrum is shown for clarity reasons. Spectra of other types of samples are comparable.

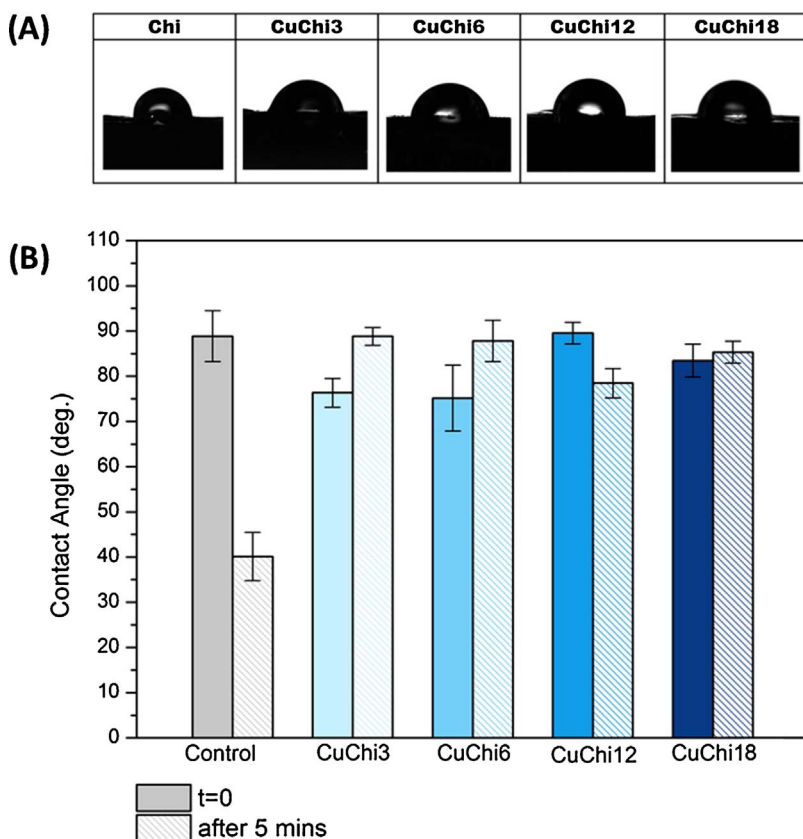


Fig. 4. (A) Profiles of water droplets on chitosan doped with increasing quantities of copper from left to right. Chitosan gels (first on the left) have been used as control. (B) Average contact angle of water droplets on CuChiX samples according to copper(II) content measured at two time-points (i.e. immediately after deposition and after 5 min).

control. For the two samples richest in Cu (i.e. *CuChi12* and *CuChi18*) the cells are mostly round shaped, a clear evidence of cell stress. Specifically, the samples doped with 12% of copper are characterized by a high total number of stained cells with an unsatisfying morphology, indicating that the cells are still alive but stressed by the copper-rich environment. Further, the staining of cells on *CuChi18* specimens is poor, leading to the conclusion that cells died at this high Cu levels. These results indicate a threshold of Cu(II) ion content (i.e. between 6 and 12% of free amino groups of chitosan) below which copper doped chitosan does not exhibit cytotoxicity and thus is a suitable candidate for biomedical applications.

3.4. Bacterial culture

All type of samples showed a strong antibacterial effect compared to a chitosan control within 9 h of inoculation (Fig. 6). Contrary to reports in the literature (No, Young Park, Ho Lee, & Meyers, 2002; Raafat & Sahl, 2009), no intrinsic bacterial inhibition through direct contact due to the chitosan itself was measured in the present study: no reduction in bacterial growth on bare chitosan was observed. The antibacterial activity of chitosan is a very delicate characteristic and the result can be a consequence of the specific DDA and molecular weight of chitosan or of the environmental conditions (e.g. the pH) not being suitable. On the contrary, the presence of copper inhibited the growth of both Gram-positive and -negative bacteria after only one hour, reaching an almost complete bacteria killing within 9 h. The finding that already low concentrations of copper have an inhibitory effect is very important since it opens up to the possibility of finding a window of effect within which the modified chitosan inhibits bacteria without significantly harming mammal cells.

4. Discussion

Copper(II)-chitosan complexes were fabricated by adapting several

previously reported protocols (Guibal et al., 2014; Mekahlia & Bouzid, 2009; Wang et al., 2005). A series of four materials was prepared incorporating copper (II) ions in amounts corresponding to theoretical molar ratios of ions to free amino-groups of chitosan ($\text{Cu}^{2+}:\text{NH}_2$) of 1:33 (*CuChi3*) and up to 1:6 (*CuChi18*). These values were chosen in order to stay significantly below the reported maximum $\text{Cu}^{2+}:\text{NH}_2$ ratio of 1:2 (Rhazi et al., 2002).

Investigation of copper(II)-chitosan complexes by SEM and optical microscopy demonstrated the reproducible fabrication of homogeneous and monophasic gels, indicating that all the copper binds to chitosan and does not form salts with other residues. In this regard, EDX spectra confirmed the absence of any unwanted residues from the reagents or apparatus used during the fabrication of the materials. Since chitosan has the inherent ability to chelate unwanted metal ions (e.g. iron, aluminum, nickel) this result is an important validation of the preparation method. EDX mapping revealed copper evenly dispersed in the matrix, thus verifying that a homogeneous embedding was achieved. In addition to this, a preliminary post-processing of the EDX data, by which the relative intensity of Cu_{KL} peaks to the $\text{C}_{\text{K}\alpha}$ peaks were calculated, showed that this relative intensity increases with increasing amounts of added copper. This result confirms that the amount of copper in the final samples can be tailored by properly dosing the amount of copper source (i.e. CuCl_2) added during synthesis. Shifts and changes in relative absorbance in the FTIR spectral bands $\nu_{\text{OH}}/\nu_{\text{NH}}$, $\nu_{\text{C=O}}$ and $\nu_{\text{N-H}}$ at 3300, 1650 and 1600 cm^{-1} respectively support that the cupric ions are coordinated via the functional amino and hydroxyl groups of the chitosan, as previously reported (Cárdenas & Miranda, 2004; Qu et al., 2011). Two models for the coordination bond are proposed in literature: a *bridge model* in which it is supposed that Cu binds various nitrogen atoms from within the same chain or from adjacent chains (Schlick, 1986) and a *pendant model* that describes the coordination as a one-to-one pendant-like bond of copper to an amino group (Ogawa, Oka, & Yui, 1993). According to other authors, these models are most probably coexisting (Rhazi et al., 2002). In the present

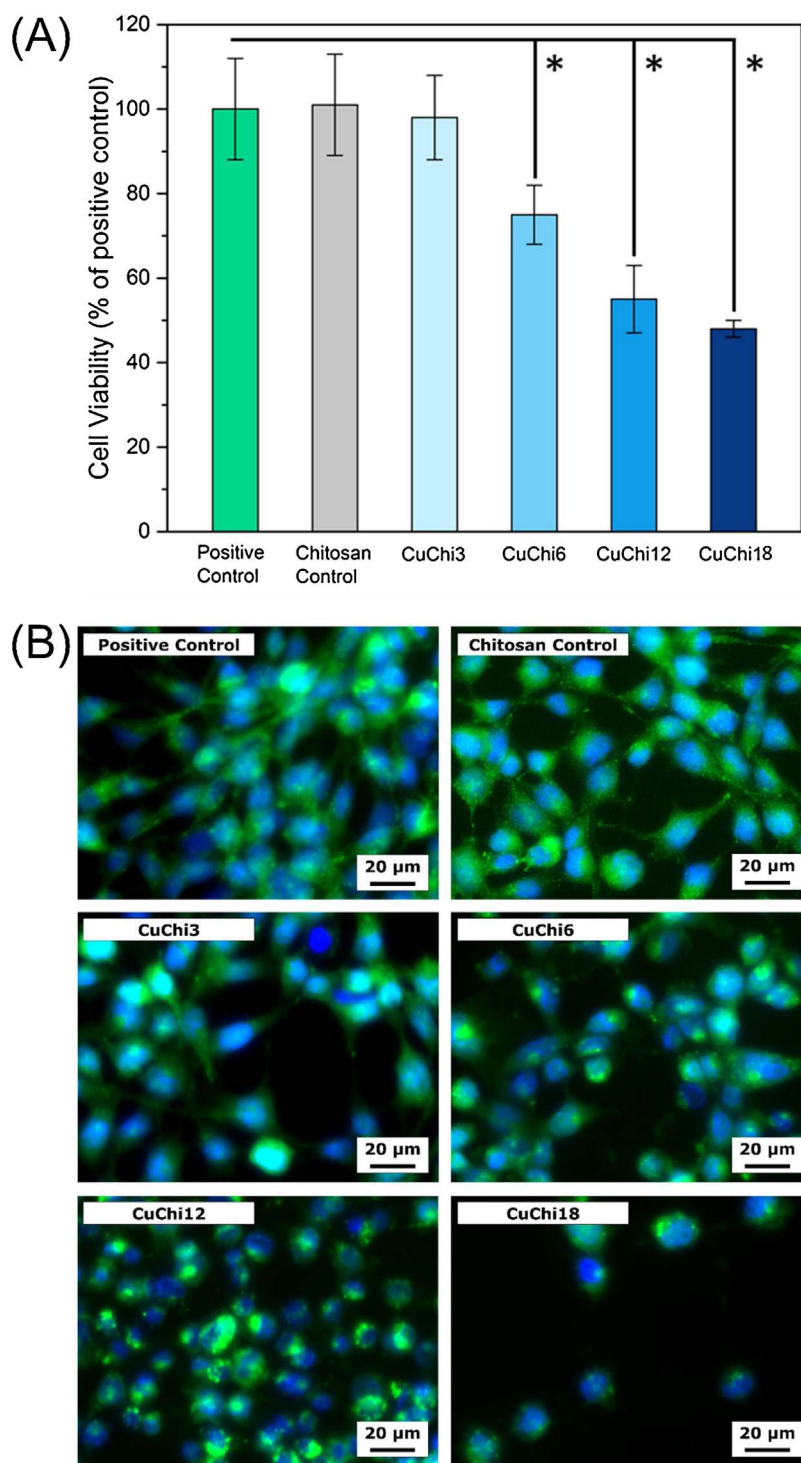


Fig. 5. (A) Histogram reporting the cell viability (WST-8 assay) of mouse embryonic fibroblasts (MEFs) cultured with each of the CuChiX samples. (B) Fluorescence microscope images showing the results of calcein-DAPI staining of MEFs after 24 h of culture with CuChiX samples. The change in morphology and consequent decrease in cell number due to the increase of copper content can be clearly seen in the CuChi12 and CuChi18 sample types (bottom row).

study, evidence supporting the first model has been found: the qualitative increase in integrity of the samples that was assessed together with the variation in the FTIR peak of the glycosidic bond (1100 cm^{-1}), suggests the occurrence of a Cu-coordinated crosslinking between different chitosan chains and supports the accuracy of the bridge model, especially when the copper ion is the bridge between amino groups of two separated polysaccharide chains (Qu et al., 2011). As already proposed by Qu et al. (Qu et al., 2011), the shape variation of the 1100 cm^{-1} peak could be due to an increased length of glycosidic bonds by steric effect due to ions within the matrix interacting with adjacent polymer chains. No significant variation in hydrophilicity was assessed via static contact angle measurements: all the samples showed

the typical mildly hydrophobic behavior of chitosan (Rivero et al., 2013). The affinity to water is reported to play a crucial role in cell adhesion and proliferation. Specifically, high wettability promotes a quicker initial response to the material, however, mildly hydrophobic substrates are reported to give better results on the longer term since they inhibit non-specific protein adsorption and allow more selected attachment to occur (Arima & Iwata, 2007).

The results on the wettability analysis combine well with the indirect MEF viability assays that were performed. They showed that for up to a $\text{Cu}^{2+}:\text{NH}_2$ ratio of 1:17 (i.e. CuChi6) the copper(II)-chitosan complexes are not harmful to MEF cells since the fibroblasts showed high viability and well-spread morphology. Most interestingly, there is

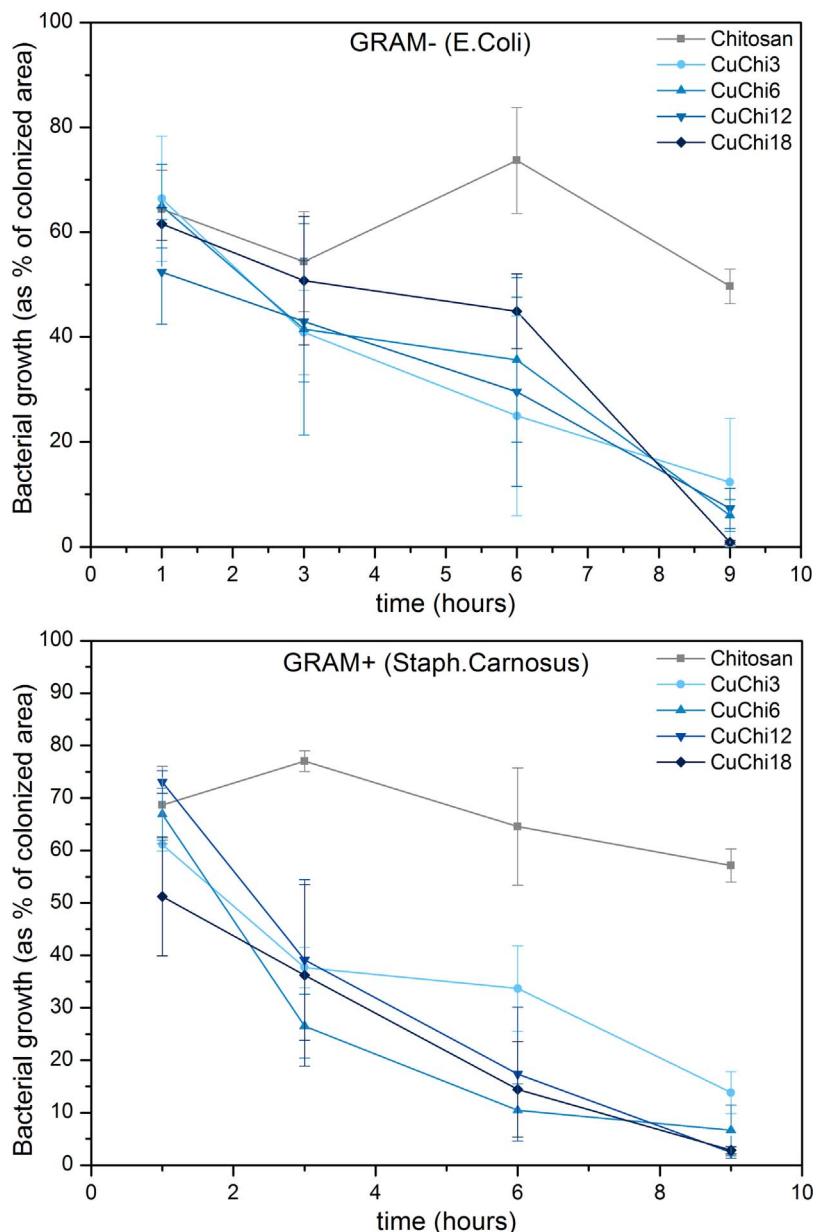


Fig. 6. The bacterial growth assessment of *Escherichia Coli* (top) and *Staphylococcus Carnosus* (bottom) on pure chitosan and copper doped chitosan shows clear inhibition due to the presence of copper. All CuChiX samples exhibit a statistically significant decrease in bacteria growth, both Gram-positive and -negative, after 9 h from inoculation.

a negative correlation between the results of cell viability assays and the quantification of copper by EDX, suggesting that the concentration of copper ions is the cause of the decrease in viability for *CuChi12* and *CuChi18*. According to previous reports, the level of copper(II) ions released in the culture medium is probably in the order of magnitude of a few tens of ppm (Rath et al., 2014; Stähli, James-Bhasin, Hoppe, Boccaccini, & Nazhat, 2015). These promising results incentivize further studies to better characterize the ion release and the response of eukaryotic cells in contact with the copper(II)-chitosan complexes. Particularly, a direct assay on mammalian cells is an important test that must be performed in order to validate the comparison between bacterial and eukaryotic cell cultures.

The assessment of the effective inhibition of bacteria by copper(II)-chitosan showed that the material, regardless of the formulation, is able to strongly reduce the growth of both the chosen strains of prokaryotes (i.e. *S. Carnosus* and *E. Coli*). A comparable effect by similarly produced copper(II)-chitosan complexes is already reported in literature against Gram negative (Mekahlia & Bouzid, 2009) and Gram positive strains (Higazy et al., 2010; Wang et al., 2005). In the present study the combination of the bacterial cultures findings with the ones of MEF cell

assays allowed the identification of an optimal range of concentration of copper that can be finely controlled adjusting the copper source and that determines fast and strong antimicrobial activity without considerably harming eukaryotic cells.

5. Conclusion

Antibacterial and cytocompatible copper(II)-chitosan complexes were prepared via *in situ* precipitation, exploiting the chelation ability of the polysaccharide and its insolubility in alkaline solutions. Copper (II)-chitosan complexes are easy to produce, cost-effective and versatile, since they can be potentially further processed using several methods to effectively implement them into biomedical devices. Preliminary feasibility studies have shown that they could be suitable materials for coatings, 3D scaffolds and electrospinning mats, among others (Guibal et al., 2014). Most importantly, the results of the biological characterizations performed on fibroblasts and Gram-positive and -negative bacteria yields both excellent cell viability and antimicrobial effect. These promising findings encourage further investigation and characterization of complexes of chitosan and therapeutic metal ions.

Future work should be focused in two main directions: (i) methodic investigation of the possible biomedical applications of the copper(II)-chitosan, particularly combining the material with other biodegradable or bioresorbable polymers as pro-angiogenic porous scaffolds and as coating of medical devices, (ii) combination of other TMIs with chitosan (e.g. calcium, zinc or strontium).

Acknowledgments

This work has received funding from the European Union's Horizon 2020 Research and Innovation Programme under the Marie Skłodowska-Curie (HyMedPoly project, Grant Agreement No. 643050) and from the German Research Foundation (DFG, Go598). We thank the HyMedPoly consortium and Ms. Astrid Mainka and Ms. Alina Grünwald for their technical assistance. We would also like to acknowledge the valuable support of Ms. Francesca Ciraldo (Institute of Biomaterials, University of Erlangen-Nuremberg).

Appendix A. Supplementary data

Supplementary data associated with this article can be found, in the online version, at <http://dx.doi.org/10.1016/j.carbpol.2017.09.095>.

References

- Arima, Y., & Iwata, H. (2007). Effect of wettability and surface functional groups on protein adsorption and cell adhesion using well-defined mixed self-assembled monolayers. *Biomaterials*, 28(20), 3074–3082. <http://dx.doi.org/10.1016/j.biomaterials.2007.03.013>.
- Cárdenas, G., & Miranda, S. P. (2004). FTIR and TGA studies of chitosan composite films. *Journal of the Chilean Chemical Society*, 49(4), 291–295. <http://dx.doi.org/10.4067/s0717-97072004000400005>.
- Guibal, E., Vincent, T., & Navarro, R. (2014). Metal ion biosorption on chitosan for the synthesis of advanced materials. *Journal of Materials Science*, 49(16), 5505–5518. <http://dx.doi.org/10.1007/s10853-014-8301-5>.
- Guibal, E. (2004). Interactions of metal ions with chitosan-based sorbents: a review. *Separation and Purification Technology*, 1, 43–74. <http://dx.doi.org/10.1016/j.seppur.2003.10.004>.
- Higazy, A., Hashem, M., Elshafei, A., Shaker, N., & Hady, M. A. (2010). Development of antimicrobial jute packaging using chitosan and chitosan-metal complex. *Carbohydrate Polymers*, 79(4), 867–874. <http://dx.doi.org/10.1016/j.carbpol.2009.10.011>.
- International Copper Association (ICA), <http://antimicrobialcopper.org>. (Accessed in January 2017).
- Kim, S. (2011). *Chitin, chitosan, oligosaccharides and their derivatives*. i–xxii. <http://dx.doi.org/10.1201/EBK1439816035>.
- Kong, M., Chen, X. G., Xing, K., & Park, H. J. (2010). Antimicrobial properties of chitosan and mode of action: a state of the art review. *International Journal of Food Microbiology*, 144(1), 51–63. <http://dx.doi.org/10.1016/j.ijfoodmicro.2010.09.012>.
- Liverani, L., Lacina, J., Roether, J. A., Boccardi, E., Killian, M. S., Schmuki, P., ... Boccaccini, A. R. (2017). Incorporation of bioactive glass nanoparticles in electrospun PCL/chitosan fibers by using benign solvents. *Bioactive Materials*. <http://dx.doi.org/10.1016/j.bioactmat.2017.05.003> (in press).
- Ma, Y., Zhou, T., & Zhao, C. (2008). Preparation of chitosan-nylon-6 blended membranes containing silver ions as antibacterial materials. *Carbohydrate Research*, 343(2), 230–237. <http://dx.doi.org/10.1016/j.carres.2007.11.006>.
- Mekahlia, S., & Bouzid, B. (2009). Chitosan-Copper (II) complex as antibacterial agent: Synthesis, characterization and coordinating bond- activity correlation study. *Physica Procedia*, 2(3), 1045–1053. <http://dx.doi.org/10.1016/j.phpro.2009.11.061>.
- Michael, C. A., Dominey-Howes, D., & Labbate, M. (2014). The Antimicrobial Resistance Crisis: Causes, Consequences, and Management. *Frontiers in Public Health*, 2, 145. <http://dx.doi.org/10.3389/fpubh.2014.00145>.
- Mourino, V., Cattalini, J. P., & Boccaccini, A. R. (2012). Metallic ions as therapeutic agents in tissue engineering scaffolds: An overview of their biological applications and strategies for new developments. *Journal of The Royal Society Interface*, 9(68), 401–419. <http://dx.doi.org/10.1098/rsif.2011.0611>.
- Munoz-Bonilla, A., Cerrada, M. L., & Fernandez-Garcia, M. (2014). CHAPTER 2 antimicrobial activity of chitosan in food, agriculture and biomedicine. *Polymeric materials with antimicrobial activity: from synthesis to applications*. The Royal Society of Chemistry 22–53. <http://dx.doi.org/10.1039/9781782624998-00022>.
- No, H. K., Young Park, N., Ho Lee, S., & Meyers, S. P. (2002). Antibacterial activity of chitosans and chitosan oligomers with different molecular weights. *International Journal of Food Microbiology*, 74(1–2), 65–72. [http://dx.doi.org/10.1016/S0168-1605\(01\)00717-6](http://dx.doi.org/10.1016/S0168-1605(01)00717-6).
- Nwe, N., Furuike, T., & Tamura, H. (2009). The mechanical and biological properties of chitosan scaffolds for tissue regeneration templates are significantly enhanced by chitosan from *Gongronella butleri*. *Materials*, 2(2), 374–398. <http://dx.doi.org/10.3390/ma2020374>.
- O'Brien, F. (2011). Biomaterials & scaffolds for tissue engineering. *Materials Today*, 14(3), 88–95. [http://dx.doi.org/10.1016/s1369-7021\(11\)70058-x](http://dx.doi.org/10.1016/s1369-7021(11)70058-x).
- O'Neill, J. (2014). Antimicrobial Resistance: Tackling a crisis for the health and wealth of nations. *Review on Antimicrobial Resistance*, 1–16. <http://dx.doi.org/10.1038/510015a>.
- Ogawa, K., Oka, K., & Yui, T. (1993). X-ray study of chitosan-transition metal complexes. *Chemistry of Materials*, 5(5), 726–728. <http://dx.doi.org/10.1021/cm00029a026>.
- Qin, Y. (1993). The chelating properties of chitosan fibers. *Journal of Applied Polymer Science*, 49(4), 727–731. <http://dx.doi.org/10.1002/app.1993.070490418>.
- Qu, J., Hu, Q., Shen, K., Zhang, K., Li, Y., Li, H., ... Quan, W. (2011). The preparation and characterization of chitosan rods modified with Fe³⁺ by a chelation mechanism. *Carbohydrate Research*, 346(6), 822–827. <http://dx.doi.org/10.1016/j.carres.2011.02.006>.
- Raafat, D., & Sahl, H. (2009). Chitosan and its antimicrobial potential – A critical literature survey. *Microbial Biotechnology*, 2(2), 186–201. <http://dx.doi.org/10.1111/j.1751-7915.2008.00080.x>.
- Rath, S. N., Brandl, A., Hiller, D., Hoppe, A., Gbureck, U., Horch, R. E., ... Kneser, U. (2014). Bioactive copper-doped glass scaffolds can stimulate endothelial cells in coculture in combination with mesenchymal stem cells. *Public library of science*, 9(12), e113319. <http://dx.doi.org/10.1371/journal.pone.0113319>.
- Rhazi, M., Desbrières, J., Tolaimate, A., Rinaudo, M., Vottero, P., & Alagui, A. (2002). Contribution to the study of the complexation of copper by chitosan and oligomers. *Polymer*, 43(4), 1267–1276. [http://dx.doi.org/10.1016/s0032-3861\(01\)00685-1](http://dx.doi.org/10.1016/s0032-3861(01)00685-1).
- Rivero, S., Garcia, M. A., & Pinotti, A. (2013). Physical and chemical treatments on chitosan matrix to modify film properties and kinetics of biodegradation. *Journal of Materials Physics and Chemistry*, 1(3), 51–57. <http://dx.doi.org/10.12691/jmpc-1-3-5>.
- Sarasam, A., & Madhally, S. V. (2005). Characterization of chitosan-polycaprolactone blends for tissue engineering applications. *Biomaterials*, 26(27), 5500–5508. <http://dx.doi.org/10.1016/j.biomaterials.2005.01.071>.
- Schlick, S. (1986). Binding sites of copper²⁺ in chitin and chitosan: An electron spin resonance study. *Macromolecules*, 19(1), 192.
- Stähli, C., James-Bhasin, M., Hoppe, A., Boccaccini, A. R., & Nazhat, S. N. (2015). Effect of ion release from Cu-doped 45S5 Bioglass® on 3D endothelial cell morphogenesis. *Acta Biomaterialia*, 19, 15–22. <http://dx.doi.org/10.1016/j.actbio.2015.03.009>.
- Sutton, S. (2011). Measurement of microbial cells by optical density. *Journal of Validation Technology*, 17(1), 46–49.
- Ventola, C. L. (2015a). The antibiotic resistance crisis: Part 1: Causes and threats. *Pharmacy and Therapeutics*, 40(4), 277–283.
- Ventola, C. L. (2015b). The antibiotic resistance crisis: part 2: management strategies and new agents. *P & T: A Peer-Reviewed Journal for Formulary Management*, 40(5), 344–352.
- Vincent, M., Hartemann, P., & Engels-Deutsch, M. (2016). Antimicrobial applications of copper. *International Journal of Hygiene and Environmental Health*. <http://dx.doi.org/10.1016/j.ijheh.2016.06.003>.
- Wang, X., Du, Y., Fan, L., Liu, H., & Hu, Y. (2005). Chitosan- metal complexes as antimicrobial agent: Synthesis, characterization and structure-activity study. *Polymer Bulletin*, 55(1), 105–113. <http://dx.doi.org/10.1007/s00289-005-0414-1>.
- Xie, H., & Kang, Y. J. (2009). Role of copper in angiogenesis and its medicinal implications. *Current Medicinal Chemistry*, 16(10), 1304–1314. <http://dx.doi.org/10.2174/092986709787846622>.